DIAGNOSTIC TOOLS FOR BEAM HALO INVESTIGATION IN SNS LINAC

A. Aleksandrov, W. Blokland, Y. Liu, C. Long, A. Zhukov.
Oak Ridge National Laboratory, Oak Ridge, TN 37830 USA

Abstract

Uncontrolled beam loss is a major concern in the operation of a high intensity hadron linac. A low density cloud of particles with large oscillation amplitudes, so called halo, can form around the dense regular beam core. This halo can be a direct or indirect cause of beam loss. There is experimental evidence of halo growing in the SNS linac and limiting the further reduction of beam loss. A set of tools is being developed for detecting of the halo and investigating its origin and dynamics. The set includes high resolution emittance measurements in the injector, laser based emittance measurements at 1 GeV, and high resolution profile measurements along the linac. We will present our experience with useful measurement techniques and data analysis algorithms.

INTRODUCTION

The SNS linac is operating routinely at beam power of about 1 MW with typical levels of uncontrolled beam loss within the design limit of 1W/m. This small level of beam loss, while considered to be acceptable, still creates significant activation of the beam line equipment, which affects the lifetime and complicates maintenance. Moreover, the SNS power upgrade plan requires a 50% increase in beam intensity while keeping uncontrolled beam loss at the present level. The major area of beam loss reduction efforts at SNS is the Super Conducting Linac (SCL). The SCL has large transverse aperture, therefore it was expected to be essentially lossless. Nonetheless, a significant beam loss was observed during commissioning and initial operation. It was discovered later that an intra-beam stripping is the main mechanism of the observed losses [1].

Intra-beam stripping losses are proportional to charge density in the bunch and, therefore, are inversely proportional to the bunch size. Increasing the bunch size is the easiest way to reduce the losses caused by the intra-beam stripping. On the other hand, the direct losses on the vacuum pipe aperture increase proportionally to the bunch size. There is an optimal beam size that can be easily calculated for a Gaussian bunch distribution. Unfortunately, as our measurements show, the bunch distribution in the SCL is not Gaussian. It consists of a dense Gaussian-like core and a less dense cloud surrounding the core. We call this cloud a "halo" without giving it a formal definition. Our goal is to reduce the number of particles in the halo or extension of the halo to allow further increase of the bunch core size.

The halo can be created at several places along the SNS linac: In the process of forming the bunches in the injector, at the transitions between the linac sections due to mismatch, and in the linac due to non-linear RF and space charge forces. Therefore, ideally, we need several measurement points to study the halo creation and propagation: at the exit of the injector, at the exit of the linac, and at as many points inside the linac as practical.

If, at this point of our study we do not understand the halo well and we do not define it quantitatively, then how do we measure it? We will use the "I know it when I see it" approach until we have sufficient understanding for developing a more sophisticated quantitative measure. In our experience, a 2-d emittance plot is a good halo visualization tool. An example of a comparison between measured emittance at 2.5MeV and at 1 GeV is shown in Fig.1. An ellipse drawn on the upper plot encloses 99% of the beam; an ellipse on the bottom plot has the same normalized area (area divided by β·γ). If the normalized emittance was conserved than the ellipse on the bottom plot would enclose 99% of the beam as well. One can clearly see that in this case there is a significant amount of beam outside of the ellipse, which looks like a low density cloud. In other words, there is a halo at 1GeV, which was not present at 2.5MeV.
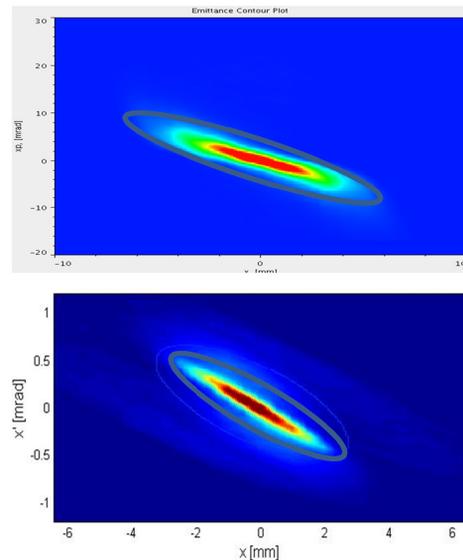
Figure 1: A comparison of two emittance measurements: one is measured at 2.5MeV (top) and the other at 1GeV (bottom). The ellipses superimposed on the images have same area in normalized coordinates.

In the next sections we will describe the tools we have or are developing to obtain the 2-d emittance plots along the SNS linac.

HALO MEASUREMENT TOOLS

The Requirements

Dynamic range and time resolution are the two major requirements for halo measurements. We do not define the halo in terms of charge density but the ultimate goal is to be able to reveal details on the level of 10^{-6}, corresponding to 1 W/m losses at 1 GeV. In the near term we set a more realistic goal of 10^4 dynamic range, which should be sufficient for studying the halo origin and behavior.

Beam in the SNS linac has a complicated time structure imposed by a fast chopper in the injector. Measurements with better than ~100ns resolution are required to study the halo variation with time. An example of the measured emittance difference between two parts of the mini-pulse, steady state and transient, is shown in Fig. 2.
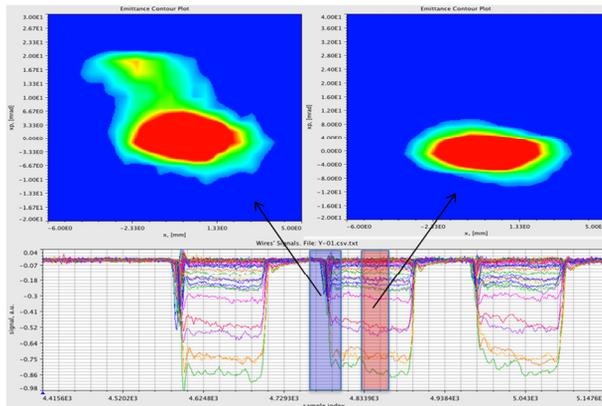
Figure 2: Emittance distortion during the chopper transient (left) revealed by a measurement with high time resolution.

Emittance Measurements in 2.5 MeV MEBT

The SNS MEBT has always had an in-line emittance measurement device of the slit-harp type [2]. Significant efforts have been applied to maximize the dynamic range and the resolution of the device. We believe that the best achieved parameters of ~1μs time resolution and ~ 10^3 dynamic ranges represent the fundamental limits of the design and cannot be further improved. Therefore a new system of the slit-slit type was developed. This device has demonstrated significantly improved time resolution of ~100ns and better than 10^3 dynamic range [2]. We believe with further improvements the time resolution can reach ~20ns the dynamic range can be higher than 10,000. These parameters allow a detailed characterization of the beam emittance in the injector, including halo.

Emittance Measurements in 1 GeV HEBT

Measuring the emittance of a hadron beam with energy in the GeV range is difficult. Fortunately, laser based diagnostics can be used in the case of H⁻ beam. We have developed a laser based system for direct measurement of 2-d emittance in the SNS HEBT at 1GeV [3]. An example

of the measurement is shown on the bottom image of Fig.1. This system has an excellent 10ns time resolution. The dynamic range of ~100 requires improvement which is the focus of our current efforts.

Reconstruction of 2-D Emittance from 1-D Profiles

There are no tools for a direct measurement of the 2-d emittance in the SNS linac between the 2.5 MeV MEBT and the 1 GeV HEBT but there is a large number of 1-d transverse profile diagnostics: Conventional wire scanners in the normal conducting linac and laser wire scanners in the super conducting linac. We are developing tomographic reconstruction techniques for re-creating 2d emittances from multiple 1-d profile measurements. The MENT algorithm works well in the HEBT, where we have a sufficient number of diagnostics in the FODO transport line as shown in Fig. 3.
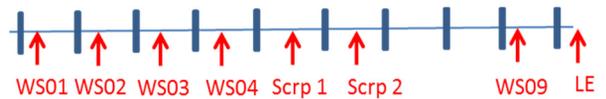
Figure 3: A layout of the HEBT lattice with diagnostics locations shown by arrows.

An example of a 2-d charge density distribution in phase space at the HEBT entrance created by the MENT algorithm is shown in Fig. 5. There is an excellent agreement between the transverse beam profiles measured by the four HEBT wire scanners (solid lines) and reconstructed by the MENT algorithm (dots) as illustrated in Fig. 4.
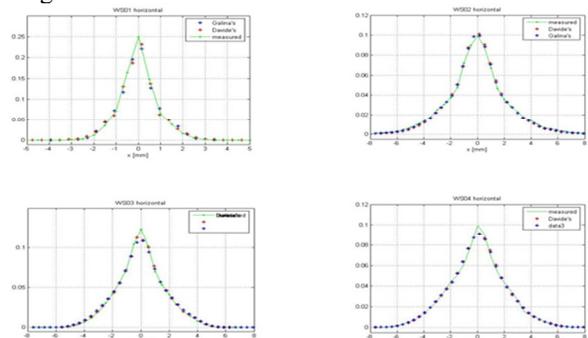
Figure 4: A comparison of transverse beam profiles measured by four HEBT wire scanners (solid lines) and reconstructed by the MENT algorithm (dots).

A comparison of a reconstructed emittance with a one measured with the laser emittance system reveals a significant difference in the distribution function shape, as illustrated by images in Fig. 6. It is interesting to note that RMS parameters of both distributions, given in the table below, are very close.

	Emittance [mm*mrad]	α	β [m]
Laser emittance	.42	2.49	15.9
MENT reconstruction	.41	2.47	13.4

Understanding of this difference is the subject of the current study.
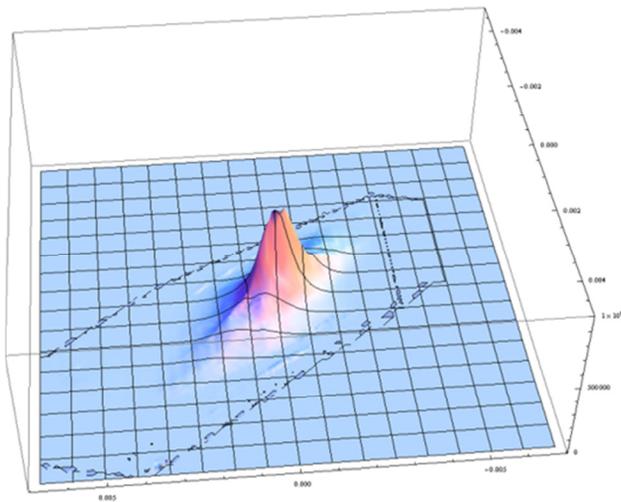
Figure 5: An example of 2-d charge distribution function reconstructed from four 1-d profiles using the MENT algorithm.
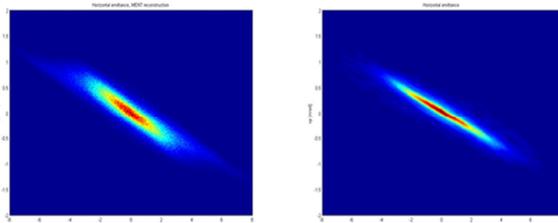
Figure 6: A comparison of charge distribution functions for the same beam: MENT reconstruction (left) and laser emittance measurement (right).
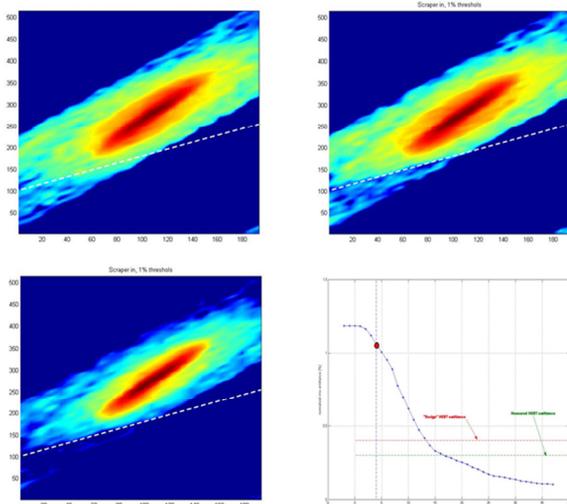
Figure 7: An example of the threshold determination for background subtraction in noisy emittance data using the upstream HEBT scraper (as explained in the text).

Use of Scrapers for Halo Study

We have several sets of scarpers in several locations along the SNS accelerator. The primary goal of the scrapers is to reduce the uncontrolled losses by intercepting stray particles (i.e. eliminating the halo). We found the scrapers to be useful for our halo study as well.

One example is finding the threshold for background subtraction in noisy emittance measurements. This is particularly important for the laser emittance measurements, which currently have a relatively large level of noise. The procedure is illustrated in Fig. 7, where top left image shows the emittance measured with an upstream scraper retracted, and the top right image shows the emittance measured with the scraper inserted. There is a shadow of the scraper clearly seen on the image. Also there is a background noise visible in the shadowed area. The threshold is increased until that background disappears as shown on the bottom left image. The bottom right plot in Fig. 7 shows a dependence of the emittance vs. the threshold, which is often used to find the proper threshold level. There are no distinct features on the curve near the correct threshold, and therefore this method is not reliable for identifying the proper threshold setting.

Another useful application is scraping the beam in the injector and observing propagation of the shadow along the linac. An example of such measurement using the wire scanners and the MENT reconstruction is shown in Fig. 8. The beam is scraped from one side in the MEBT as seen on the bottom left image. The measured distribution in the HEBT is shown on the right image. There is no a visible asymmetry or shadow. The distribution is completely homogenized during the process of acceleration.
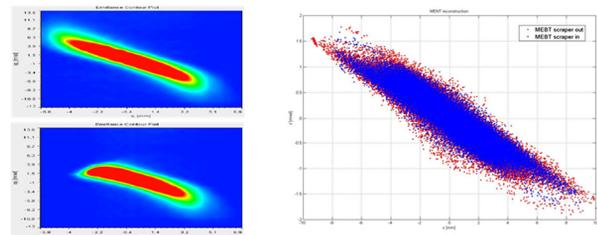
Figure 8: An example of measuring scraper shadow propagation along the linac. Explanation is in the text.

ACKNOWLEDGEMENTS

REFERENCES

[1] G. Galambos, et al, these proceedings.

[2] A. Zhukov, et.al, these proceedings.

[3] Y. Liu, et al., NIM A 675 (2012) 97–102.